RESEARCH LETTER

blood advances

TO THE EDITOR:

Restored biosynthetic pathways induced by MSCs serve as rescue mechanism in leukemia cells after L-asparaginase therapy

Natividad Alquezar-Artieda,[1,2] Daniela Kuzilkova,[1-3] Jennie Roberts,[4] Katerina Hlozkova,[1,2] Alena Pecinova,[5] Petr Pecina,[5] Martina Zwyrtkova,[1,2] Eliska Potuckova,[1,2] Daniel Kavan,[6] Ivana Hermanova,[1,2] Marketa Zaliova,[1-3] Petr Novak,[6] Tomas Mracek,[5] Lucie Sramkova,[2,3] Daniel A. Tennant,[4] Jan Trka,[1-3] and Julia Starkova[1-3]

[1]Childhood Leukaemia Investigation Prague, Prague, Czech Republic; [2]Second Faculty of Medicine, Department of Pediatric Hematology and Oncology, Charles University, Prague, Czech Republic; [3]University Hospital Motol, Prague, Czech Republic; [4]Institute of Metabolism and Systems Research, College of Medical and Dental Sciences, University of Birmingham, Birmingham, United Kingdom; [5]Department of Bioenergetics, Institute of Physiology of the Czech Academy of Science, Prague, Czech Republic; and [6]Laboratory of Structural Biology and Cell Signalling, Institute of Microbiology, Academy of Science of the Czech Republic, Prague, Czech Republic

L-asparaginase (ASNase), the drug included on the World Health Organization's list of essential medicines, is irreplaceable in the front-line treatment of childhood acute lymphoblastic leukemia (ALL).[1] However, the relapse of ALL[2,3] is often associated with resistance[4] to ASNase and its mechanisms are not fully understood. The cytotoxic effect of ASNase relies on depleting exogenous asparagine (Asn) and glutamine (Gln), inducing apoptosis in leukemic cells because of their reduced capability of Asn synthesis.[5] Our previous in vitro data demonstrated that ASNase triggers metabolic reprogramming of leukemic cells, which impedes the anti-leukemic effect.[6] Metabolic processes of leukemic cells have been shown to be altered by the environment of the bone marrow (BM), which may contribute to chemoresistance.[7-12] Herein, we investigated the impact of BM attributes on cellular metabolic processes of leukemic cells in order to demonstrate the more complex picture[13] of ASNase-driven metabolic rewiring and its role in the mechanism of resistance.

First, we explored the effect of ASNase on leukemic cell survival in the experimental model established in this study. The model mimics the BM environment of patients with ALL undergoing ASNase treatment, which was achieved using transient ASNase treatment that resembles an inherent elimination of the drug in vivo, a coculture with mesenchymal stromal cells (MSCs) that partially simulates the BM matrix (supplemental Figure 1A-E)[14,15] and hypoxic conditions.[16,17] Four B-cell precursor (BCP)-ALL cell lines (NALM-6, REH, RS4-11, and SUP-B15) in the presence and absence of MSCs were treated with different concentrations of transient ASNase treatment. After 96 and 120 hours of ASNase treatment, the survival of all tested leukemic cell lines in coculture was significantly increased compared with that in monoculture (Figure 1A; supplemental Figure 1F). Interestingly, the survival of the cocultured leukemic cells following ASNase treatment in hypoxia was comparable to the effect under normoxic conditions (Figure 1B; supplemental Figure 1G-H). The prosurvival effect of MSCs on leukemic cells after ASNase treatment was also recapitulated in primary cells, observed in 4 of 7 patients whose cells were isolated from BCP-ALL diagnosis (supplemental Figure 1I). In addition, the protective effect of MSCs was also observed when using alternatives for the BM scaffold as HS-5, a fibroblast-like cell line with similar progenitor potential,[18] and primary MSCs, isolated from pediatric patients with BCP-ALL (supplemental Figure 1J-K).

Next, we investigated the changes in bioenergetic and biosynthetic pathways after 48 hours of ASNase treatment.[19] We previously showed a metabolic rewiring of leukemic cells after ASNase treatment, resulting in glycolysis reduction (via glucose uptake measurement [GU]) and fatty acid oxidation (FAO) elevation.[6] Herein, we showed that ASNase-induced changes in bioenergetic metabolism persist in the presence of MSCs. Measuring GU, we detected similar changes in the mono and cocultures of

Submitted 26 October 2021; accepted 7 November 2022; prepublished online on *Blood Advances* First Edition 18 November 2022; final version published online 15 May 2023. https://doi.org/10.1182/bloodadvances.2021006431.

Data are available on request from the corresponding author, Julia Starkova (julia.starkova@lfmotol.cuni.cz).

The full-text version of this article contains a data supplement.

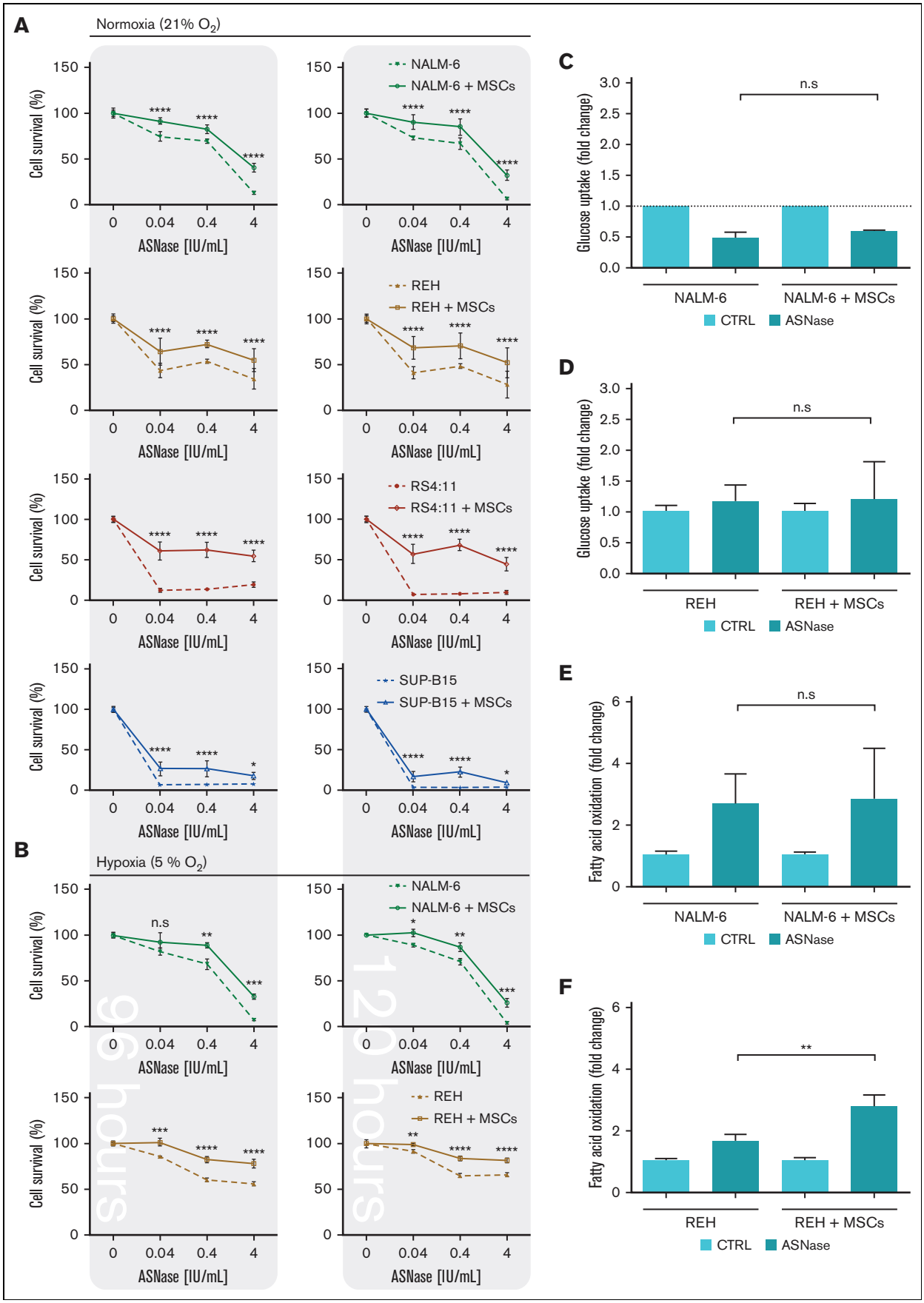

Figure 1.

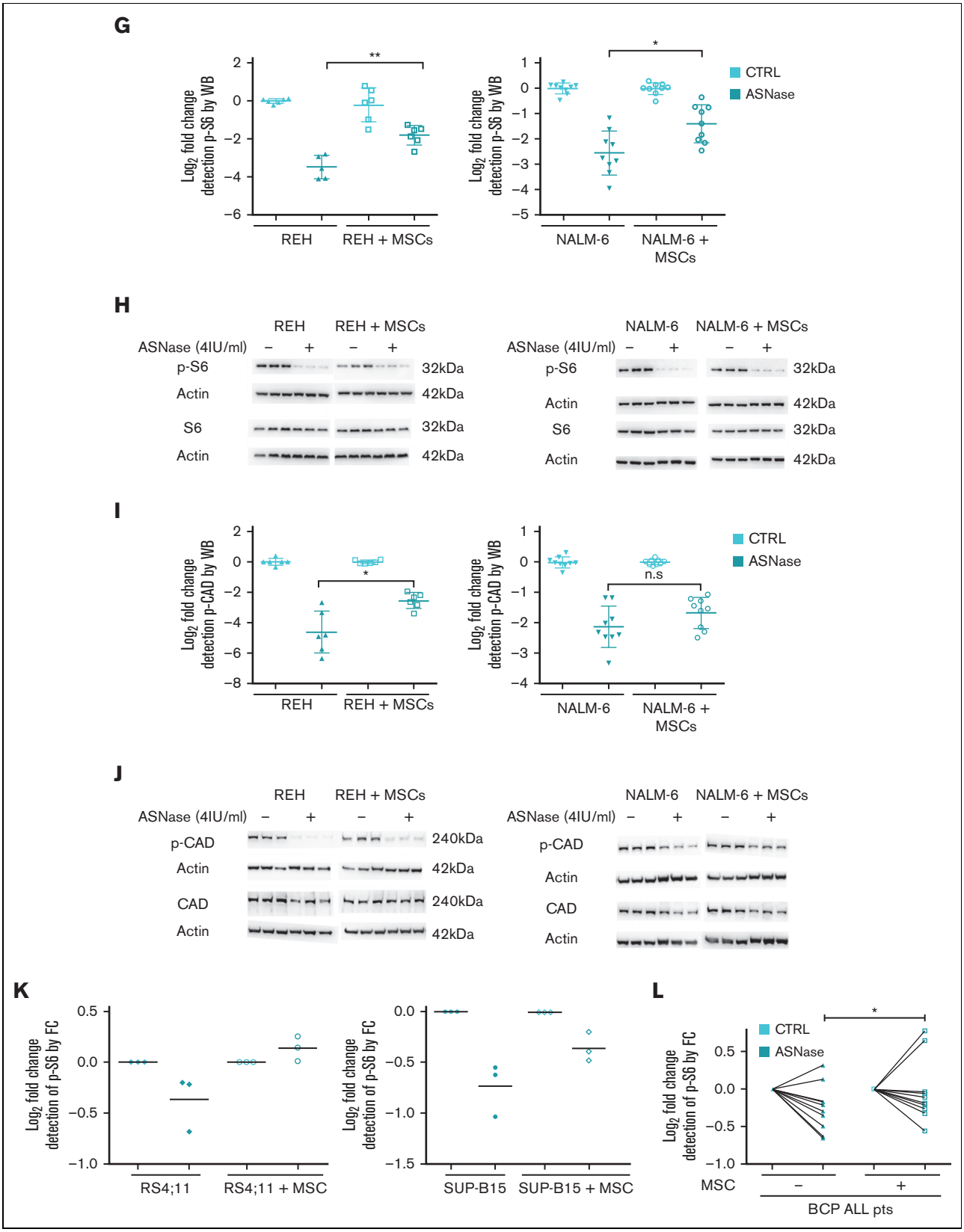

Figure 1 (continued)

NALM-6 cell line (Figure 1C). REH cells did not decrease GU in either presence or absence of MSCs, in line with previously published data showing milder changes in GU in this cell line[6] (Figure 1D). FAO significantly increased in both cell lines independent of MSCs' presence, having significantly higher levels in REH cells in the coculture than those in the monoculture (Figure 1E-F). We assume it is caused by the higher energy demand required to sustain the increase of biosynthetic processes that depend uniquely on FAO because other bioenergetic sources (glucose, Gln) are shut down.[20] Biosynthetic pathways were explored by analyzing mTOR, the mechanistic target of rapamycin (RAPA) pathway, as the major nutrient-sensitive regulator.[21] We previously showed that ASNase in vitro inhibits the mTOR signaling pathway in leukemic cells and its downstream targets.[6] Herein, we observed the inhibition of p-S6 in leukemia cells after the ASNase treatment in both cultures. However, the inhibition was significantly less prominent in the coculture model (Figure 1G-K; supplemental Figure 1L). Partial reactivation in the presence of MSCs was also detected in the phosphorylation of CAD (p-CAD), another downstream protein of mTOR complex 1 (mTORC1)/S6K1 (prevalent in REH cells; Figure 1I-J).[22,23] Furthermore, we also observed the partial restoration of p-S6 induced by MSCs in primary leukemic cells upon ASNase treatment, detected in 9 of 11 analyzed patients with statistical significance (Figure 1L). These results suggested the contribution of MSCs in the reactivation of protein (p-S6) and nucleotide (p-CAD) synthesis, regulated by mTOR.

Downstream signaling of mTORC1 responds to extracellular Asn,[6,24] which could be released from MSCs. To elucidate the hypothesis, we measured the flux of Asn using stable isotope tracing and assessed the activity of de novo Asn synthesis in MSCs followed by the efflux of Asn to culture media (Figure 2A). MSCs were first cultivated without Asn and with 15N-Gln for 7 days, resulting in 50% labeled intracellular Asn (Figure 2B). Next, we transferred MSCs (with labeled intracellular Asn) to a medium simulating the ASNase effect and detected extracellular Asn from which 11.67% ± 0.57 was labeled (M+1) after 48 hours of incubation, confirming the efflux of Asn from MSCs (Figure 2C). We also verified 94% of intracellular Asn (M+6) were taken in by leukemic cells in both monoculture and coculture using $15N_2$-$13C_4$-Asn in culture media (Figure 2D). These data confirmed that Asn is replenished in the presence of MSCs, which are supported by the increased levels of p-S6 and p-CAD proteins in leukemic cells incubated with increasing Asn concentrations and without Gln (Figure 2E-G). Moreover, increased cell proliferation correlated with increased levels of Asn (Figure 2H). Importantly, the extent of the described phenomenon is different for each cell line because of their specific intrinsic factors (cell proliferation, doubling time, and basal metabolic profile).

In order to test if Asn supplementation from MSCs hinders ASNase sensitivity via mTOR restoration, we treated leukemic cells in monoculture and coculture with a combination of either 0.4 IU/mL or 4 IU/mL of ASNase and 25nM of RAPA (supplemental Figure 1M), an mTOR inhibitor.[25] The combination of RAPA and 0.4 IU/mL of ASNase diminished the prosurvival effect of MSCs in both NALM-6 and REH cell lines. REH cells also showed similar results using 4 IU/mL of ASNase and RAPA. This effect was not observed in NALM-6, suggesting a more complex mechanism given its resistant phenotype to ASNase. Moreover, in lower concentrations of ASNase, RAPA decreased the survival of NALM-6 and REH in monoculture as well (Figure 2I-J). These results confirmed that the mTOR pathway plays a crucial role in the rescue mechanism induced by MSCs on leukemic cells upon ASNase treatment.

Because Asn deficiency is reflected in the induced mRNA levels of *ASNS*, we assessed *ASNS* gene expression in the presence and absence of MSCs as well as the expression of *CHOP*, a product of amino acid stress response, and the amino acid transporters *SLC38A2*, *SLC7A1*, and *SCL1A4*.[26,27] After ASNase treatment, the expression of all studied genes was induced only in the monoculture of both leukemic cell lines. In contrast, the gene expression was unchanged in the coculture, confirming the amino acids deficit in the monoculture (Figure 2K; supplemental Figure 2A-B). Furthermore, we asked how Asn deficiency influenced the transport of other amino acids. Amino acids flow analysis showed a significant (mostly gradual) increase in the uptake of most of the amino acids after ASNase treatment in monoculture. The increase in amino acid uptake was less prominent in cocultured leukemic cells following ASNase treatment (Figure 2L; supplemental Figure 2C).

Our previously published results on metabolic rewiring in leukemic cells after ASNase treatment were obtained in purely in vitro conditions in which ASNase was constantly present in the culture and did not reflect the pharmacokinetics of the in vivo administration.

Figure 1. Rescued leukemic cells by the coculture model upon ASNase treatment showed restored p-S6 and p-CAD. (A-B) Growth assay of leukemic cells by flow cytometry. Leukemic cell lines were seeded in the presence and absence of MSCs and cultured with increasing concentrations of transient ASNase treatment for a specific time. After determining the absolute number of cells, the results were normalized to untreated samples and presented as the percentage of cell survival. Each symbol of the survival line represents the mean ± SD from (A) 3 independent experiments performed in biological triplicates and (B) a biological triplicate experiment. (C-F) Leukemic cells (NALM-6; REH) in mono and cocultures were cultured with transient ASNase treatment (4 IU/mL) for 48 hours, then GU measurement (C-D) and FAO measurement (E-F) were performed. Bar graphs represent the mean ± SD of the results in fold change normalized to the untreated sample from at least 2 independent experiments performed in biological triplicates. $^{**}P$-value = .0043. (G-J) mTOR activity analysis by detecting the phosphorylated form of its downstream proteins (S6 and CAD) using western blotting. Leukemic cells in mono and cocultures were cultured with 4 IU/mL of transient ASNase treatment for 48 hours (NALM-6) or 72 hours (REH). The results were quantified and normalized to β-actin, presented as the log2 fold change relative to that of untreated samples. Every point of the dot plot represents the result of each biological triplicate from the n = 2 to 3 independent experiments. (G) p-S6 protein quantification (REH, $^{**}P$-value = .0043; and NALM-6, $^{*}P$-value = .0106). (H) p-S6, S6 and β-actin of a representative western blot. (I) p-CAD protein quantification ($^{*}P$-value = .0152), (J) p-CAD, CAD and β-actin of a representative western blot. (K-L) Results from the phosphorylated form of S6 measured by spectral cytometry in leukemic cells. Approximately 4.00E+06 leukemic cells, either cell lines (RS4:11 and SUP-B15, K) or primary cells (L), were seeded in the presence and absence of MSCs (2.00E+05 cells per 24mm insert transwell) and cultured with 4 IU/mL of transient ASNase treatment for 8 (K, L) and 24 hours (L). Two-way ANOVA (pairwise comparison; A-B), two-tailed Mann-Whitney test (D-J) and Wilcoxon test (K) were used to determine statistically significant differences. $^{*}P < .05$, $^{**}P < .01$ $^{***}P < .001$, $^{****}P < .0001$. ANOVA, analysis of variance; CTRL, control; FC, flow cytometry; n.s, not significant; p-S6, phosphorylated S6 ribosomal protein; p-CAD, phosphorylated CAD; WB, western blot.

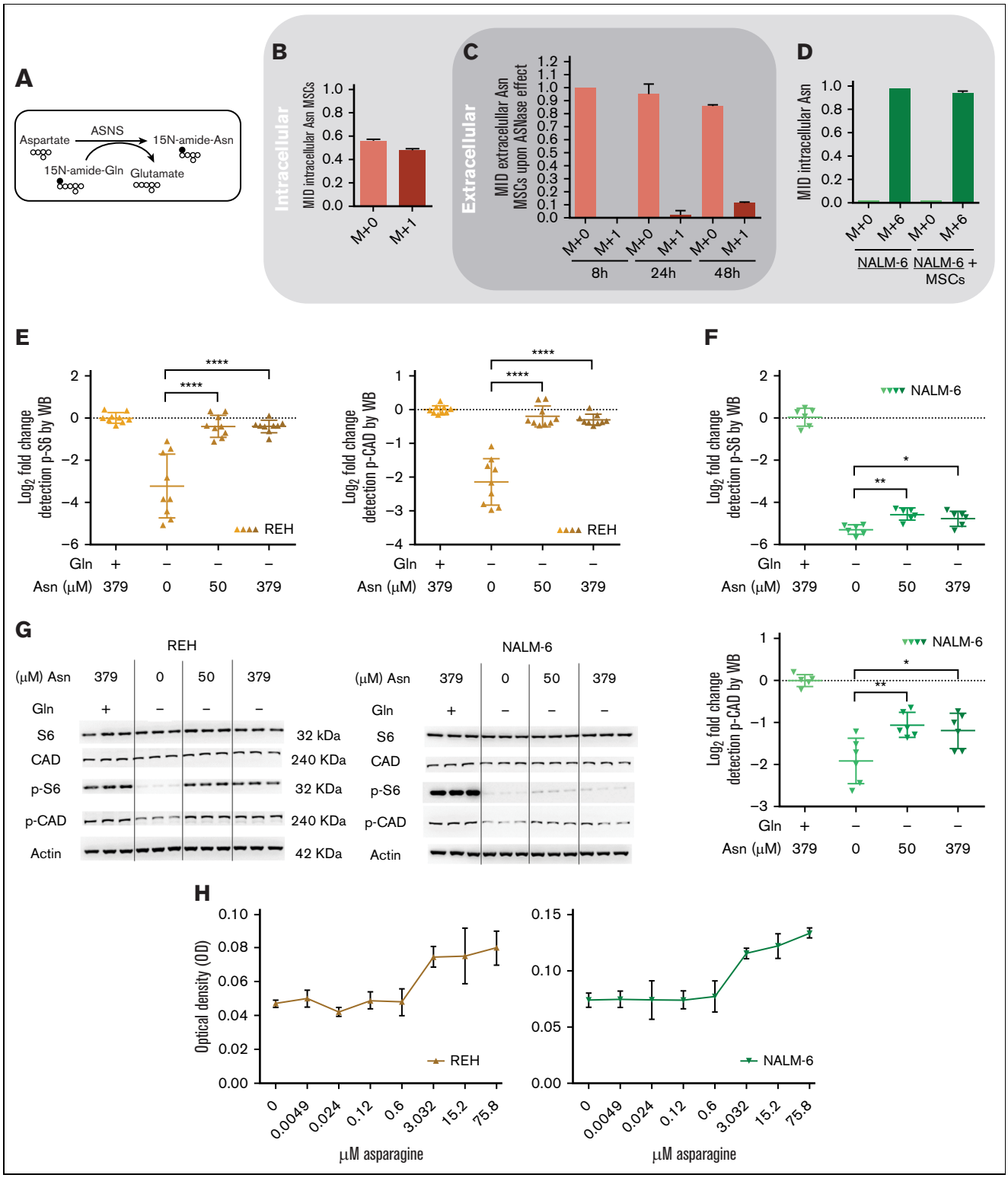

Figure 2. MSCs from the coculture model *de novo* synthesized and released Asn, which mitigated ASNase-nutrient stress and restored p-S6 and p-CAD in leukemic cells. (A-D) Detection of the efflux of de novo synthesized Asn from MSCs to the media using SIT with N15-amide-Gln. Each bar graph represents the results as mean ± SD of MID from a biological triplicate experiment. (A) Scheme of de novo Asn synthesis showing the transfer of the labeled isotope from N15-amide-Gln to N15-amide-Asn (M+1). (B) MID of intracellular Asn in MSCs cultured with free Asn complete medium supplemented with N-amide-Gln for 7 days. This complete medium was prepared from a modified RPMI lacking Gln, Asn, Glu and Asp, which was supplemented then with 2 mM of N-amide-Gln, 150 μM of Asp and 136 μM of Glu. (C) MID of Asn in the medium (extracellular Asn) simulating ASNase effect cultured with MSCs for specific time-points. This medium was prepared using the modified RPMI mentioned in (B), supplemented with a reduced concentration of Gln (500 μM), 528 μM Asp and 2.136 mM Glu. The last 2 concentrations were adjusted from technical RPMI formulation assuming the

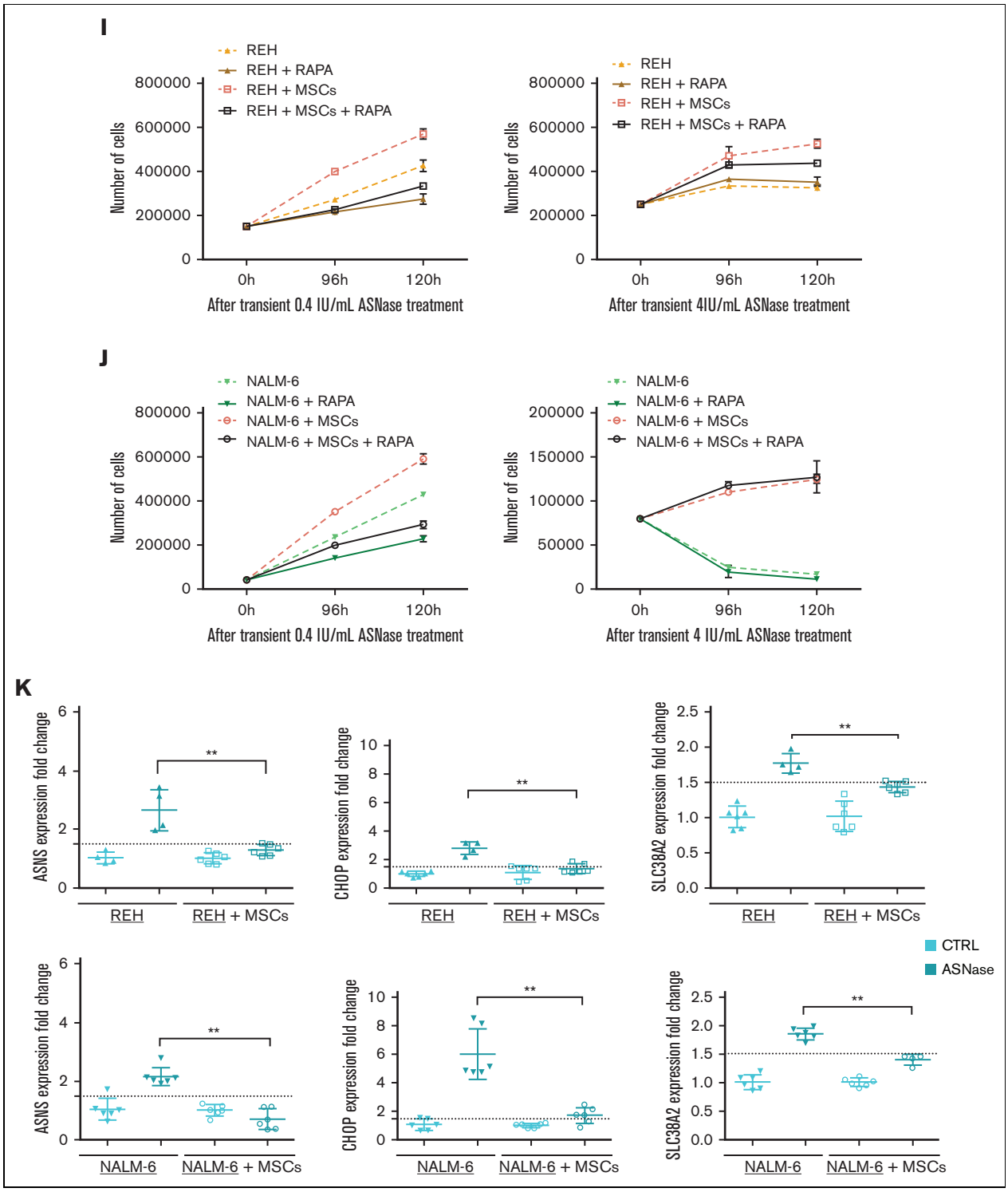

Figure 2 (continued) complete conversion (1:1) due to the action of ASNase on Asn and Gln to Asp and Glu. The reduced Gln concentration ensured the pathways' stability, avoiding the labeled isotope loss in Asn. (D) MID of intracellular Asn in NALM-6 in mono and cocultures after 24 hours of culture with Gln-free medium (the modified RPMI, B) supplemented with 15N2-13C4-Asn (379 μM), 150 μM Asp and 136 μM Glu. (E-F) mTOR activity analysis in REH and NALM-6 cells by detecting the phosphorylated form of its downstream protein (S6 and CAD) using western blotting. Leukemic cells (7.50E + 05 cells per mL) were cultured with a medium (the modified RPMI, B) simulating the ASNase effect (0 Gln, 528 μM Asp, and 2.136 mM Glu), supplemented with increasing concentrations of Asn for 24 hours. The results were quantified and normalized to β-actin, presented as the log2 fold change relative to that of untreated samples. Every point of the dot plot represents the result of each biological triplicate from the n = 2 to 3 independent experiments. (G) p-S6, S6, p-CAD, p-CAD and β-actin of a representative western blot. (H) Cell proliferation of leukemic cells using MTS assay. Leukemic cells were cultured with a medium simulating the ASNase effect mentioned in (E), supplemented with increasing Asn concentrations for 72 hours. The results are shown in OD, and symbols represent

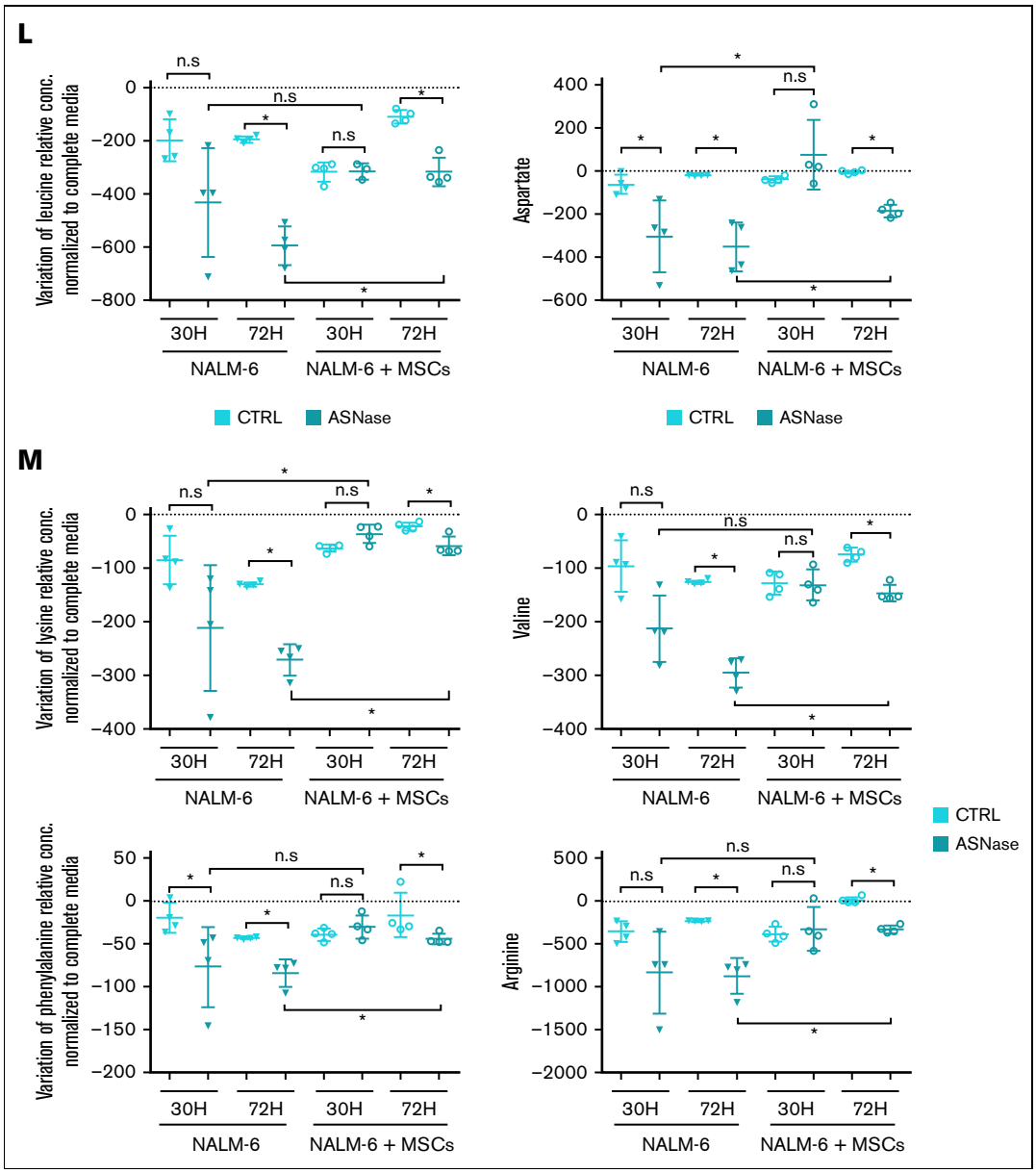

Figure 2 (continued) the means ± SD results from n = 1 to 3 independent experiments in 6 biological replicates. (I-J) Growth assay of leukemic cells undergoing transient ASNase treatment combined or not with 25nM of rapamycin (RAPA). Each symbol on the curve represents the mean ± SD from a biological triplicate experiment. (K) Relative quantification of the expression of ASNS, CHOP, and SLC38A2 using qPCR. The gene expression was measured in leukemic cells (underlined cell line represents the one analyzed) in the presence and absence of MSCs cultured with 4 IU/mL of transient ASNase treatment for 6 hours. Results were normalized to the average of 2 housekeepers' genes and calculated the fold change to untreated samples per time point and condition. Each symbol of the dot plot represents the result of each duplicate measurement from n = 1 to 2 independent experiments in a biological triplicate. ASNS, *P*-value = .0095 (REH) and *P*-value = .0022 (NALM-6); CHOP, *P*-value = .0095 (REH) and *P*-value = .0022 (NALM-6); SLC38A2, *P*-value = .0095 (REH) and *P*-value = .0095 (NALM-6). The dotted line marks a fold change of 1.5. (L) The flux of extracellular amino acids was determined by high-performance liquid chromatography (HPLC) in mono and coculture models. NALM-6 cells (0.30E + 06 cells per mL) were seeded with or without MSCs and cultured with 4 IU/mL transient ASNase treatment for 30 and 72 hours. The culture media were collected to determine amino acid concentrations. Results were normalized following a two-step process; (1) Extraction of the amino acid concentrations in complete medium at time 0 and (2) normalization of the amino acid concentrations to the number of cells. This normalization allows us to distinguish the direction of the amino acid flow; influx and efflux are represented as values below and above zero (marked with a dotted line), respectively. Each symbol represents the result of each replicate from a biological quadruplicate experiment. Two-tailed Mann-Whitney test was assessed to determine statistically significant differences between 2 groups. $^{*}P < .05$, $^{**}P < .01$, $^{****}P < .0001$. ASNS, asparagine synthetase; MID, mass isotopologue distribution; n.s, not significant; OD, optical density; qPCR, quantitative polymerase chain reaction.

Additionally, leukemic cells were cultured without any scaffold characteristic of the BM environment.[6] In this study, we used a more relevant in vitro model considering the main aspects of the BM environment. Using this model, we confirmed the survival advantage of leukemic cells in the presence of MSCs when comparing proliferation and viability with those of common in vitro cultures. Additionally, culturing the cells at different oxygen concentrations did not affect survival. Surprisingly, the change in bioenergetic pathways was similar to that in monoculture, supporting the relevance of our previous findings and showing that the presence of MSCs does not affect ASNase-driven metabolic reprogramming.[6] Furthermore, we showed that Asn was de novo synthesized in MSCs and released into the Asn-free culture media, reactivating p-S6 and p-CAD. This event prompted leukemic cells to proliferate even in the presence of ASNase, the effect that was diminished using an mTOR inhibitor, RAPA. The amino acid stress caused by Asn depletion, represented by elevated levels of *ASNS*, *SLC38A2*, *CHOP*, *SLC7A1*, and *SLC1A4* and an increased amino acid uptake was compensated in coculture.

To our knowledge, this study is the first to demonstrate that protein and nucleotide synthesis participate in the MSCs-mediated chemoresistance to ASNase treatment. Our results show that MSCs sustain biosynthetic pathways in leukemic cells, making them more accessible to bioenergetic rewiring, which may counteract ASNase cytotoxicity. These results bring us closer to a better understanding of the mechanism of action of common cytostatic drugs and unravel survival mechanisms that could help to develop novel treatment options to improve the outcome for patients with ALL.

Acknowledgments: This work was supported by the Grant Agency of Czech Republic (GAČR no: 20-27132S), the project National Institute for Cancer Research (Programme EXCELES, ID project number LX22NPO5102), funded by the European Union NextGenerationEU and by the Ministry of Health, Czech Republic, and the conceptual development of research organization, Motol University Hospital, Prague, Czech Republic 00064203. N.A.-A. was supported by the grant agency of Charles University, nr.794218. A.P. was supported by the Grant Agency of Czech Republic (GAČR no: 21-18993S). The figures were created with BioRender.com.

Contribution: N.A.A. optimized and performed cell cultivation models and flow cytometry; J.R., K.H., and D.A.T. designed and performed stable isotope tracing; N.A.A. and D. Kuzilkova performed assays with patients with ALL; N.A.A., I.H., A.P., P.P., and T.M. optimized and performed glucose uptake and FAO; N.A.A. and E.P. performed protein isolation and western blot; N.A.A. and M. Zwyrtkova performed RNA isolation and qPCR; D. Kavan and P.N. performed high-performance liquid chromatography analysis; L.S. and J.T. were responsible for collection of patient samples and isolation of primary leukemic cells; J.S. designed the project and coordinated the study; J.S., N.A.A., K.H., J.T., and M. Zaliova wrote the manuscript and analyzed the data; and all the authors revised the manuscript and approved the final version.

Conflict-of-interest disclosure: The authors declare no competing financial interests.

ORCID profiles: P.P., 0000-0003-0641-2834; D.K., 0000-0003-2693-1199; M.Z., 0000-0002-1639-7124; T.M., 0000-0002-9492-0718; D.A.T., 0000-0003-0499-2732; J.T., 0000-0002-9527-8608; J.S., 0000-0002-2269-5849.

Correspondence: Julia Starkova, Second Faculty of Medicine, Dept.of Pediatric Hematology and Oncology, Charles University, V Uvalu 84, 15006 Prague, Czech Republic; email: julia.starkova@lfmotol.cuni.cz.

References

1. Pui C, Evans WE. Treatment of acute lymphoblastic leukemia. *N Engl J Med*. 2006;354(2):166-178.
2. Einsiedel HG, Von Stackelberg A, Hartmann R, et al. Long-term outcome in children with relapsed ALL by risk-stratified salvage therapy: results of trial acute lymphoblastic leukemia-relapse study of the Berlin-Frankfurt-Münster group 87. *J Clin Oncol*. 2005;23(31):7942-7950.
3. Nguyen K, Devidas M, Cheng SC, et al. Factors influencing survival after relapse from acute lymphoblastic leukemia: a children's oncology group study. *Leukemia*. 2008;22(12):2142-2150.
4. Iacobucci I, Mullighan CG. Genetic basis of acute lymphoblastic leukemia. *J Clin Oncol*. 2017;35(9):975-983.
5. Tabe Y, Lorenzi PL, Konopleva M. Amino acid metabolism in hematologic malignancies and the era of targeted therapy. *Blood*. 2019;134(13):1014-1023.
6. Hermanova I, Arruabarrena-Aristorena A, Valis K, et al. Pharmacological inhibition of fatty-acid oxidation synergistically enhances the effect of l-asparaginase in childhood ALL cells. *Leukemia*. 2016;30(1):209-218.
7. Polak R, De Rooij B, Pieters R, den Boer ML. B-cell precursor acute lymphoblastic leukemia cells use tunneling nanotubes to orchestrate their microenvironment. *Blood*. 2015;126(21):2404-2414.
8. Ede BC, Asmaro RR, Moppett JP, Diamanti P, Blair A. Investigating chemoresistance to improve sensitivity of childhood T-cell acute lymphoblastic leukemia to parthenolide. *Haematologica*. 2018;103(9):1493-1501.
9. Ehsanipour EA, Sheng X, Behan JW, et al. Adipocytes cause leukemia cell resistance to l-asparaginase via release of glutamine. *Cancer Res*. 2013;73(10):2998-3006.
10. Pillozzi S, Masselli M, De Lorenzo E, et al. Chemotherapy resistance in acute lymphoblastic leukemia requires hERG1 channels and is overcome by hERG1 blockers. *Blood*. 2011;117(3):902-914.
11. Sison EAR, Brown P. The bone marrow microenvironment and leukemia: biology and therapeutic targeting. *Expert Rev Hematol*. 2011;4(3):271-283.
12. Ma L, Zong X. Metabolic symbiosis in chemoresistance: refocusing the role of Aerobic glycolysis. *Front Oncol*. 2020;10:1-8.
13. Meyer LK, Hermiston ML. The bone marrow microenvironment as a mediator of chemoresistance in acute lymphoblastic leukemia. *Cancer Drug Resist*. 2019;2(4):1164-1177.
14. Manabe A, Coustan-Smith E, Behm FG, Raimondi SC, Campana D. Bone marrow-derived stromal cells prevent apoptotic cell death in B- lineage acute lymphoblastic leukemia. *Blood*. 1992;79(9):2370-2377.
15. Iwamoto S, Mihara K, Downing JR, Pui CH, Campana D. Mesenchymal cells regulate the response of acute lymphoblastic leukemia cells to asparaginase. *J Clin Invest*. 2007;117(4):1049-1057.

16. Muz B, de la Puente P, Azab F, Azab AK. The role of hypoxia in cancer progression, angiogenesis, metastasis, and resistance to therapy. *Hypoxia (Auckl)*. 2015;3:83-92.

17. Fecteau JF, Messmer D, Zhang S, et al. Impact of oxygen concentration on growth of mesenchymal stromal cells from the marrow of patients with chronic lymphocytic leukemia. *Blood*. 2013;121(6):971-974.

18. Adamo A, Delfino P, Gatti A, et al. HS-5 and HS-27A stromal cell lines to study bone marrow mesenchymal stromal cell-mediated support to cancer development. *Front Cell Dev Biol*. 2020;8:584232.

19. Cai J, Wang J, Huang Y, et al. ERK/Drp1-dependent mitochondrial fission is involved in the MSC-induced drug resistance of T-cell acute lymphoblastic leukemia cells. *Cell Death Dis*. 2016;7(11): e2459-11.

20. Gonzalez-Manchon C, Parrilla R, Ayuso MS. Role of fatty acid in the control of protein synthesis in liver cells. *Biochem Int*. 1990;21(5): 933-940.

21. Melick CH, Jewell JL. Regulation of mTORC1 by upstream stimuli. *Genes (Basel)*. 2020;11(9):1-28.

22. Robitaille AM, Christen S, Shimobayashi M, et al. Quantitative phosphoproteomics reveal mTORC1 activates de novo pyrimidine synthesis. *Science*. 2013;339(6125):1320-1323.

23. Saxton RA, Sabatini DM. mTOR signaling in growth, metabolism, and disease. *Cell*. 2017;168(6):960-976.

24. Krall AS, Xu S, Graeber TG, Braas D, Christofk HR. Asparagine promotes cancer cell proliferation through use as an amino acid exchange factor. *Nat Commun*. 2016;7:11457.

25. Li J, Xue L, Hao H, et al. Rapamycin provides a therapeutic option through inhibition of mTOR signaling in chronic myelogenous leukemia. *Oncol Rep*. 2012;27(2):461-466.

26. Hellsten SV, Lekholm E, Ahmad T, Fredriksson R. The gene expression of numerous SLC transporters is altered in the immortalized hypothalamic cell line N25/2 following amino acid starvation. *FEBS Open Bio*. 2017;7(2):249-264.

27. Balasubramanian MN, Butterworth EA, Kilberg MS. Asparagine synthetase: regulation by cell stress and involvement in tumor biology. *Am J Physiol Endocrinol Metab*. 2013;304(8):E789-E799.